Air permeametry on outcrop analogues: a composite image of the Neogene aquifer, Belgium.

B. Rogiers[1,2], K. Beerten[1], T. Smekens[2],
M. Huysmans[2], M. Gedeon[1], D. Mallants[3],
O. Batelaan[2,4], A. Dassargues[2,5]

[1] SCK•CEN – [2] KU Leuven – [3] CSIRO – [4] VUB – [5] ULg

EGU 2012
24 April, 2012

Contents

Contents

- Introduction
  - Research context
  - Neogene aquifer
- Methods
- Results
- Conclusions

Research context

- Saturated hydraulic conductivity (K_s)
  - one of the most important parameters
  - determining groundwater flow and contaminant transport
  - in both unsaturated and saturated porous media
- In-situ K_s measurements
  - remain very complex and scale-dependent
  - air permeameters have being used effectively in the field as an indirect method to determine K_s
- Case study: Neogene aquifer, Belgium
  - important groundwater resource
  - subject to hydrogeological assessments in the framework of potential future disposal of radioactive waste

Neogene aquifer - Location

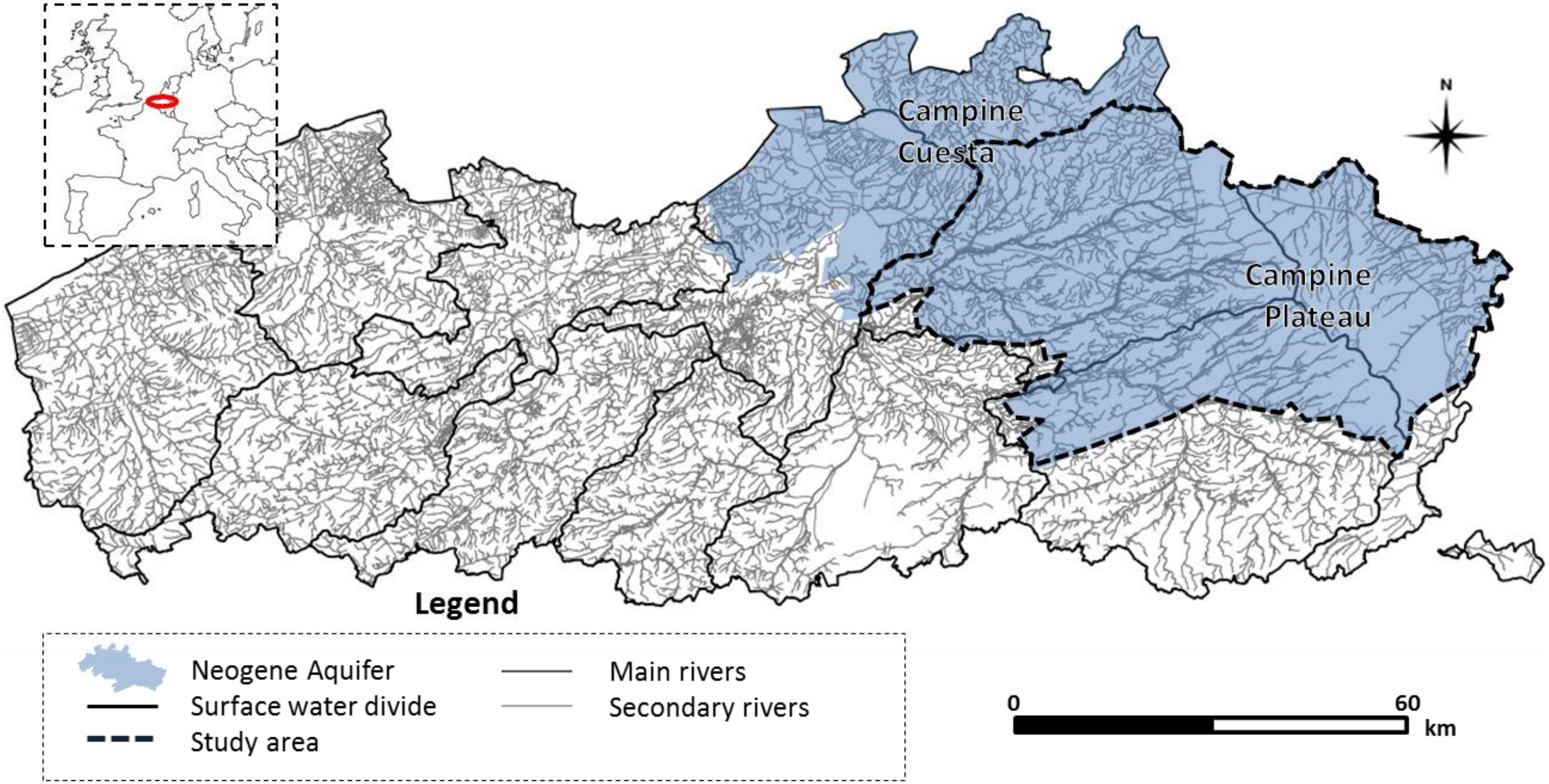

Neogene aquifer - Geology

- Coarse to fine sands
- Distinct clayey zones

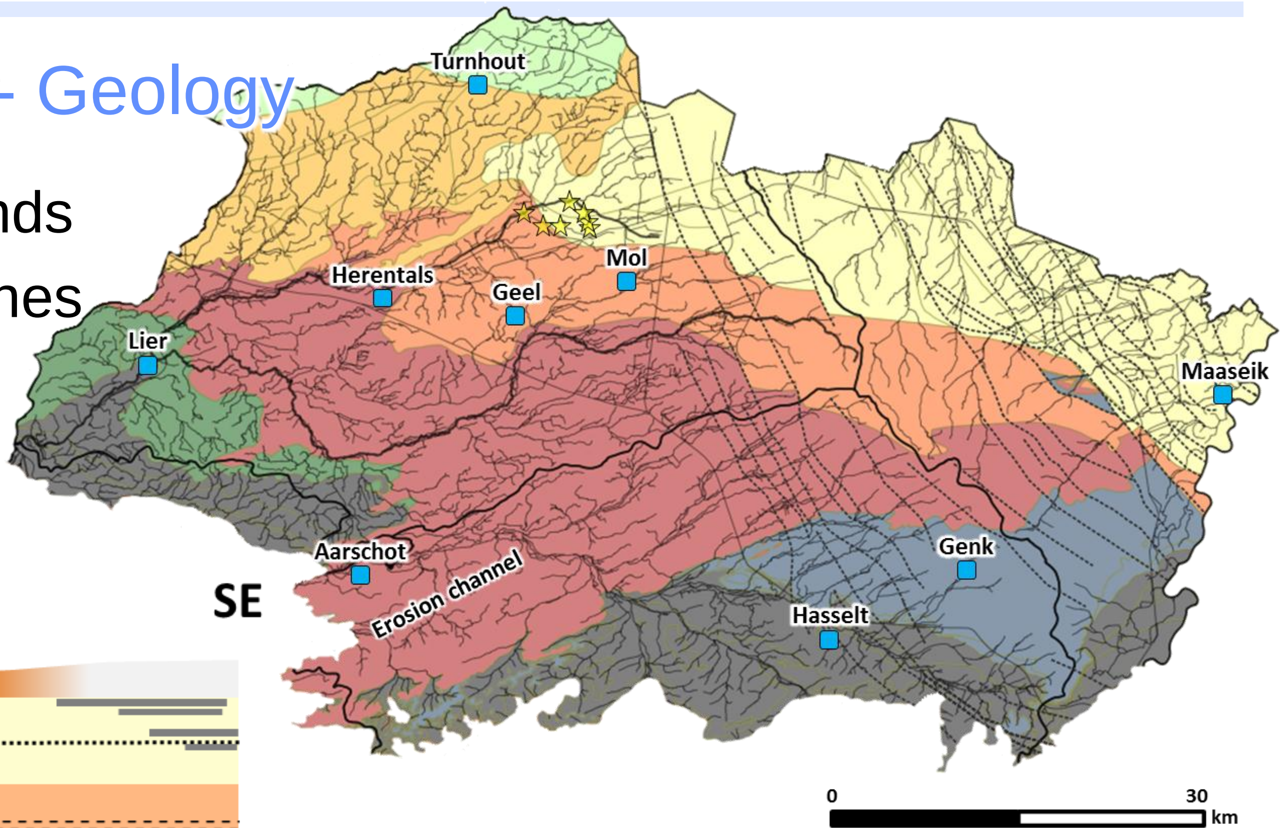

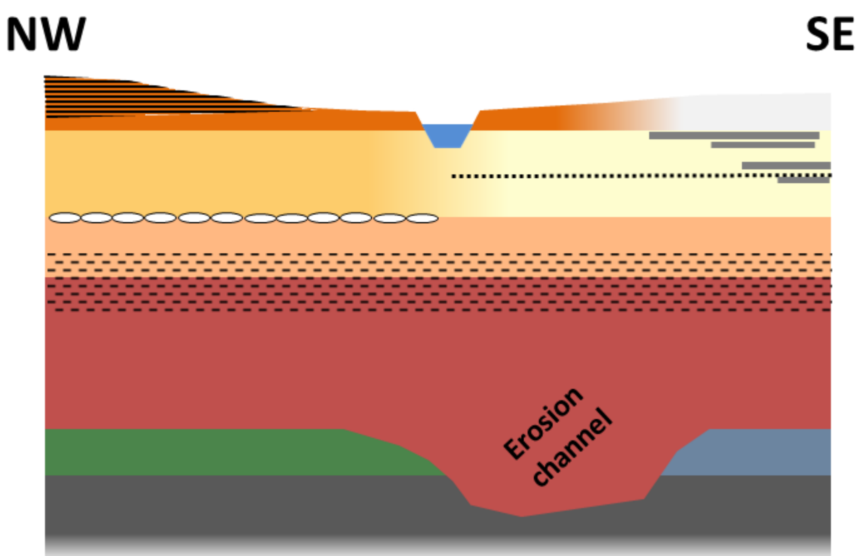

Neogene aquifer – Selected outcrops

- Availability
- Accessibility

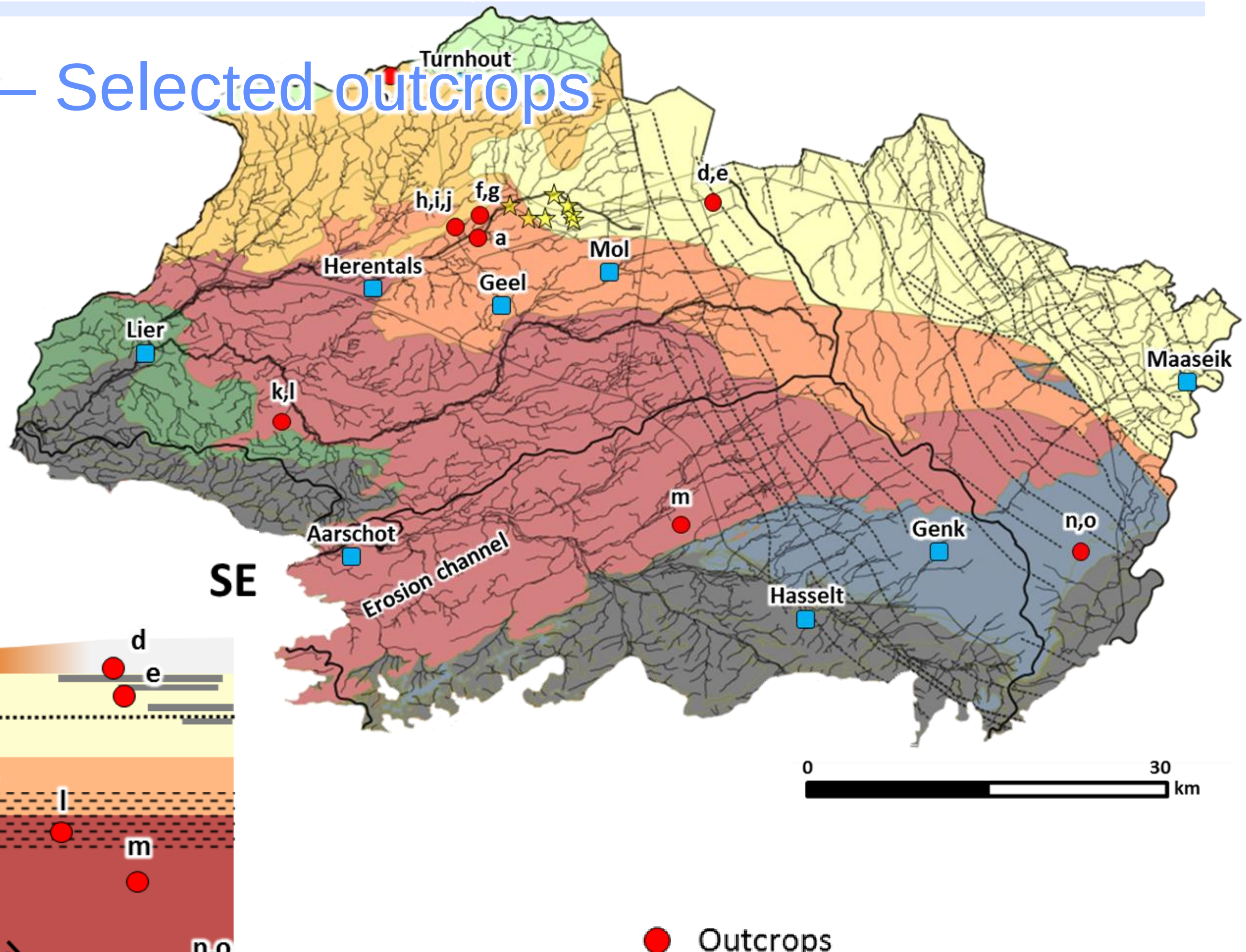

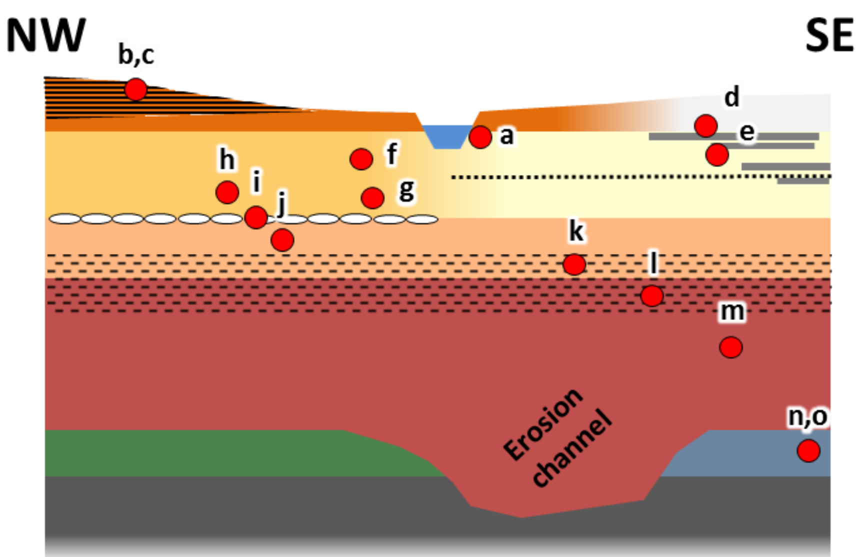

Contents

Air permeability measurements

- Tinyperm II
  air permeameter
  New England Research &
  Vindum Engineering 2011

- Equation from literature
  to convert k_a to K_s
  Iversen et al 2003

Validation in the lab

- Kopecky ring samples of different lithologies
- Constant head permeameter tests

Numerical upscaling

- Derive one single K tensor with flow conservation
- Approaches
  - Permeameter-type setup
    - Prescribed head at in- and outflow boundaries
    - No-flow at parallel boundaries

$$-\begin{bmatrix} \nabla\bar{h}_x & 0 \\ 0 & \nabla\bar{h}_z \end{bmatrix} \begin{bmatrix} K_{xx} \\ K_{zz} \end{bmatrix} = \begin{bmatrix} \bar{q}_x \\ \bar{q}_z \end{bmatrix}$$

  - Combination of 4 boundary condition setups
    - Prescribed head everywhere
    - 4 flow directions

$$-\begin{bmatrix} \nabla\bar{h}_{x1} & 0 & \nabla\bar{h}_{z1} \\ 0 & \nabla\bar{h}_{z1} & \nabla\bar{h}_{x1} \\ \nabla\bar{h}_{x2} & 0 & \nabla\bar{h}_{z2} \\ 0 & \nabla\bar{h}_{z2} & \nabla\bar{h}_{x2} \\ & \cdots & \end{bmatrix} \begin{bmatrix} K_{xx} \\ K_{zz} \\ K_{xz} \end{bmatrix} = \begin{bmatrix} \bar{q}_{x1} \\ \bar{q}_{z1} \\ \bar{q}_{x2} \\ \bar{q}_{z2} \\ \cdots \end{bmatrix}$$

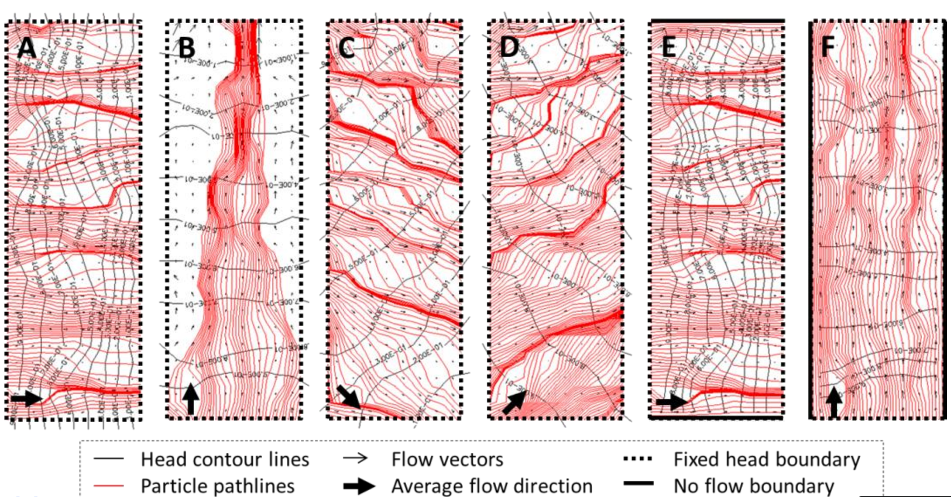

e.g. Zhou et al 2010; Li et al 2011

Contents

Air permeameter measurements

Quaternary

Pliocene

Miocene

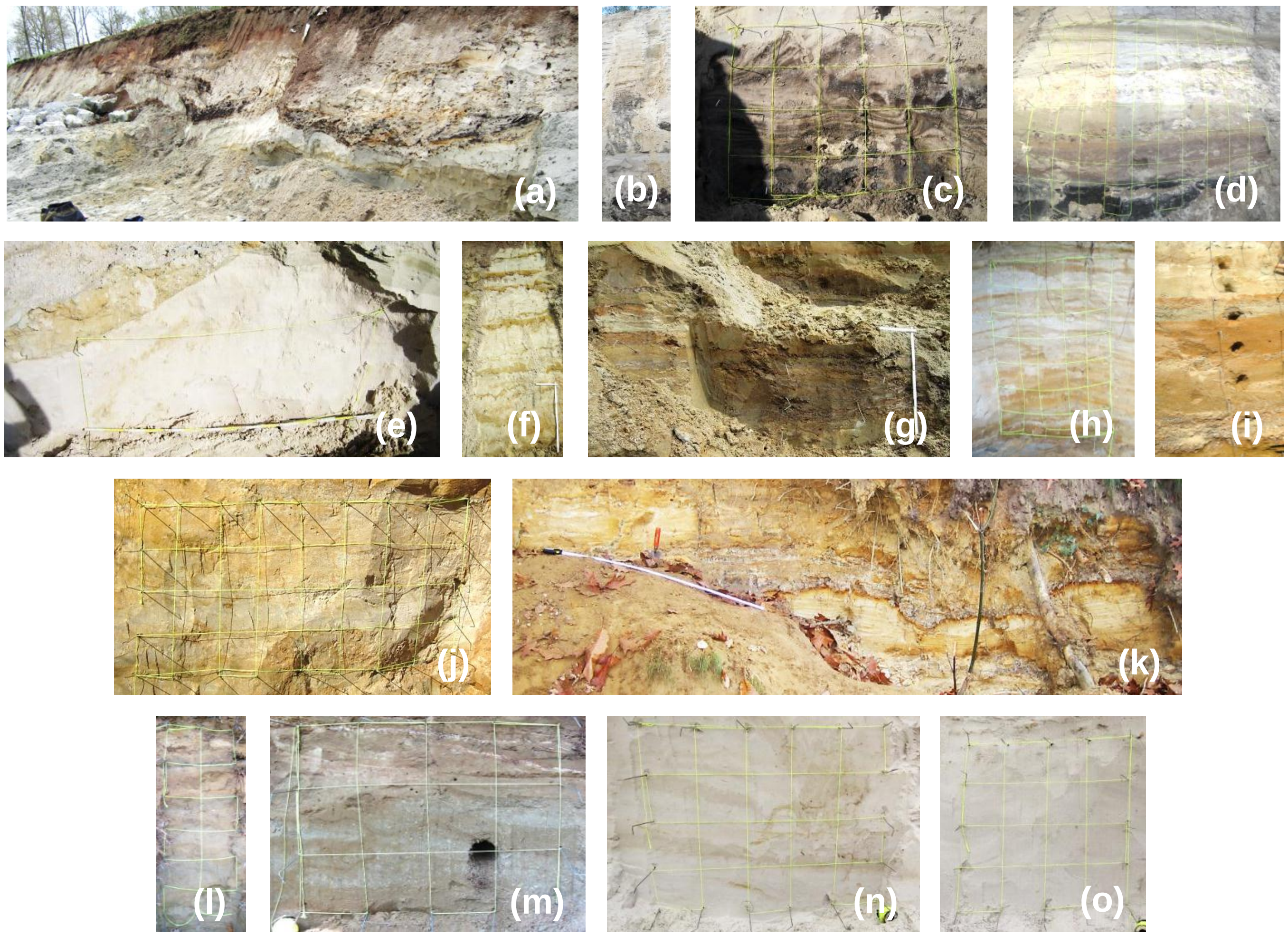

Air permeameter measurements

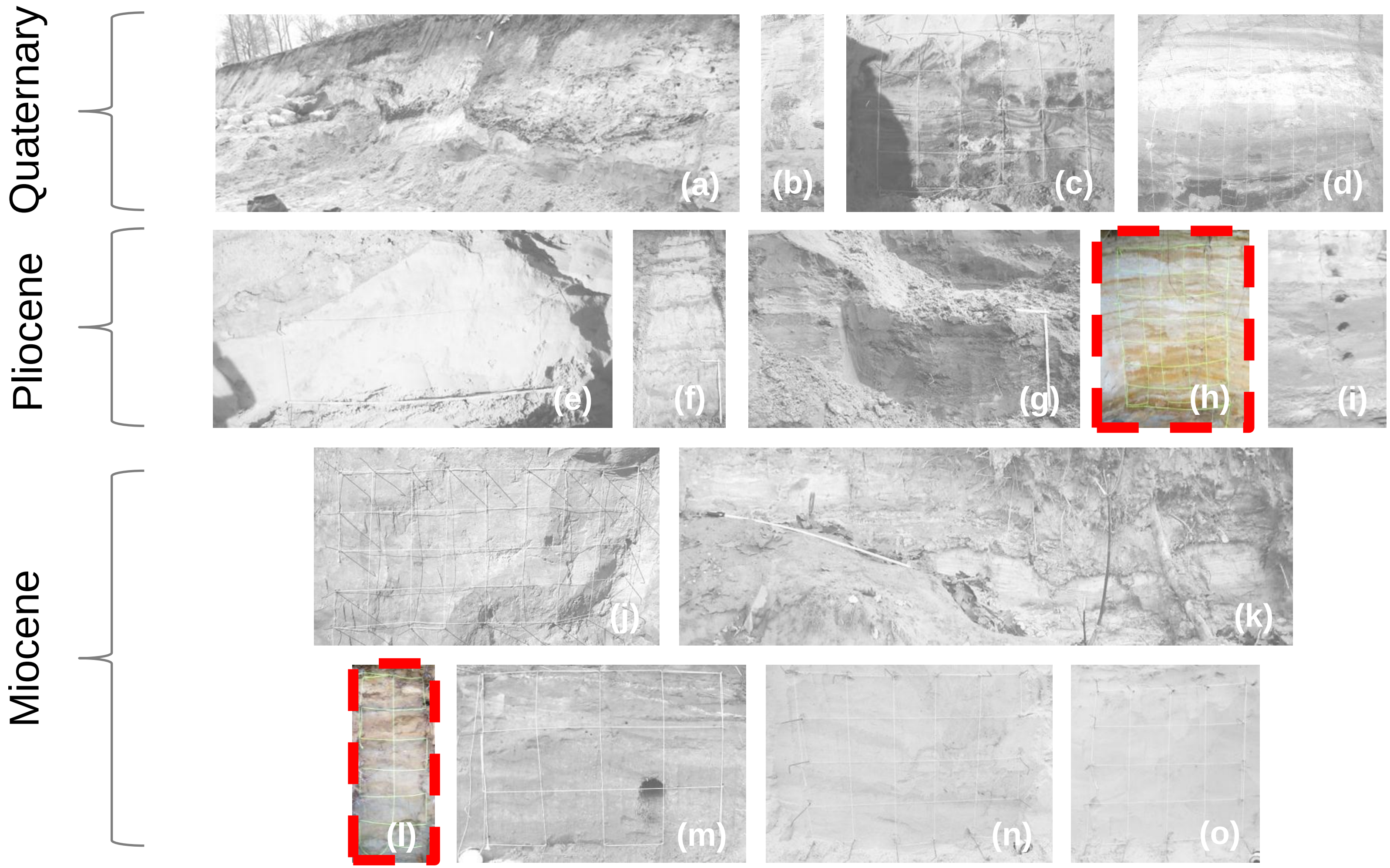

Air permeameter measurements – 2 examples

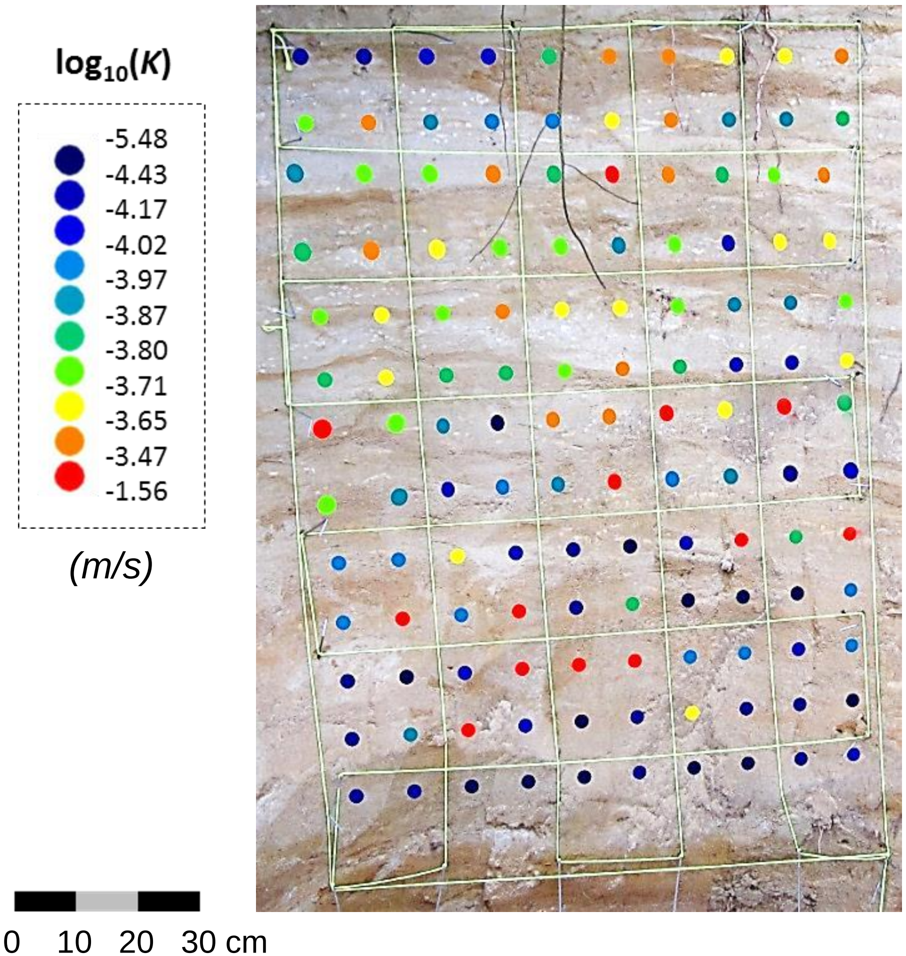

Poederlee Sands

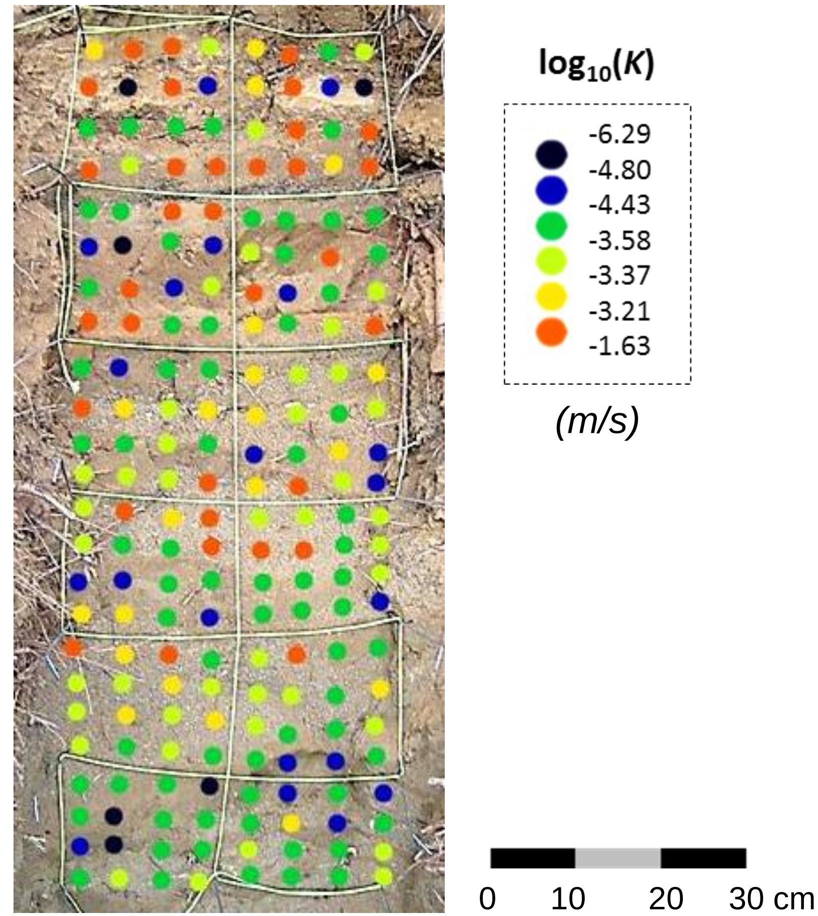

Diest Clayey Sands

Air permeameter measurements

ID	Sediment	$\log_{10}(K_s)$ *(m/s)*			
		Min	Max	Mean	Range
a	Kleine Nete point bar sands	-4.3	-3.4	-3.7	0.8
	Kleine Nete channel fill	-9.2	-8.3	-8.9	0.9
b	Campine clay-sand complex profile	-8.1	-3.6	-5.1	4.6
c	Ice wedge & cryoturbation structures	-7.8	-2.5	-4.9	5.3
d	Lommel Sands	-6.4	-2.3	-4.2	4.1
e	Mol Sands	-4.0	-3.1	-3.7	0.9
f	Top Poederlee Formation	-6.5	-3.7	-4.5	2.8
g	Bottom Poederlee Formation 1	-7.8	-4.4	-5.9	3.4
h	Bottom Poederlee Formation 2	-5.4	-1.6	-3.9	3.9
i	Hukkelberg stratigraphical boundary	-8.2	-3.7	-5.3	4.5
j	Kasterlee Sands	-6.7	-2.0	-3.9	4.6
k	Kasterlee Clay	-6.6	-2.2	-4.4	4.4
l	Clayey top Diest Formation	-6.1	-1.7	-3.7	4.5
m	Diest Sands	-5.0	-3.6	-4.1	1.3
n	Bolderberg Sands 1	-4.2	-3.5	-3.9	0.8
o	Bolderberg Sands 2	-4.3	-3.5	-3.9	0.8

Validation in the lab

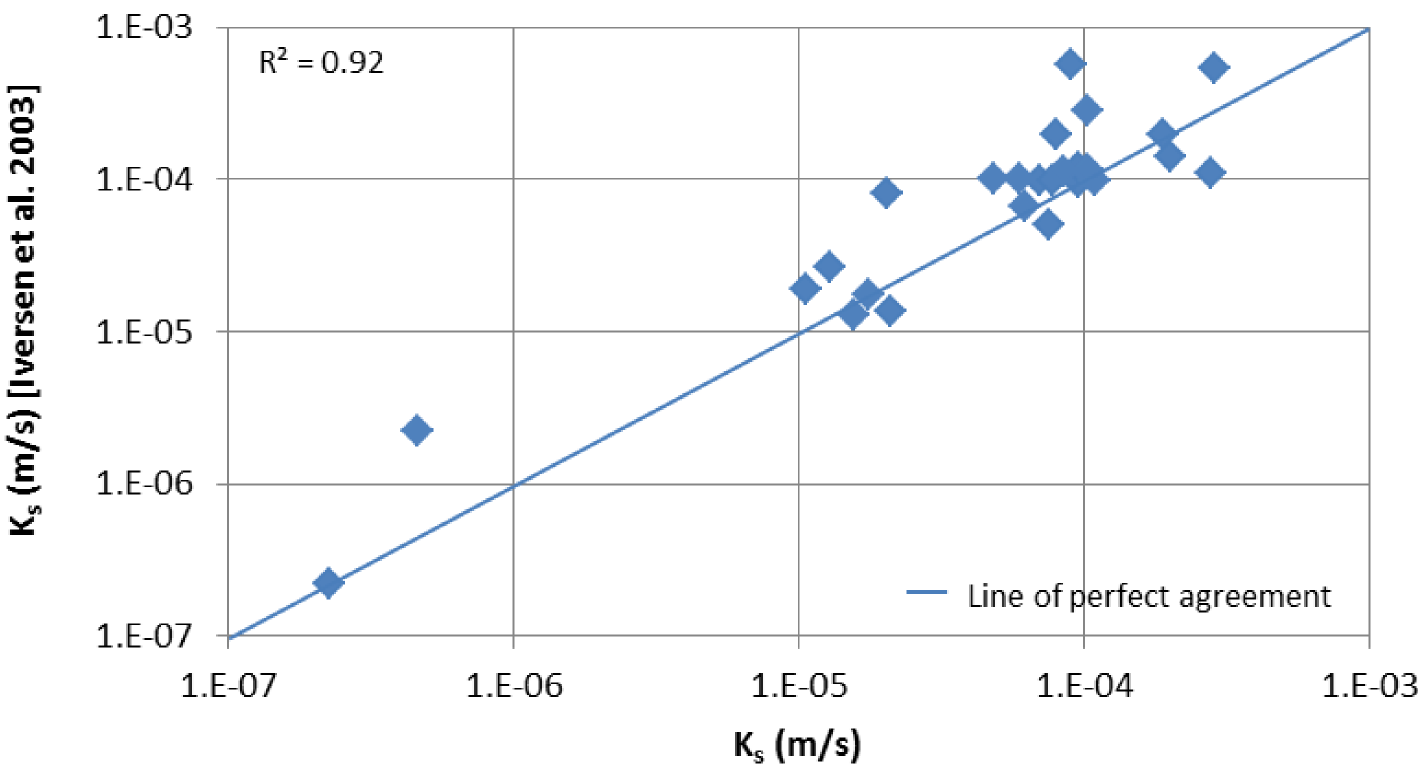

Numerical upscaling – 2 examples

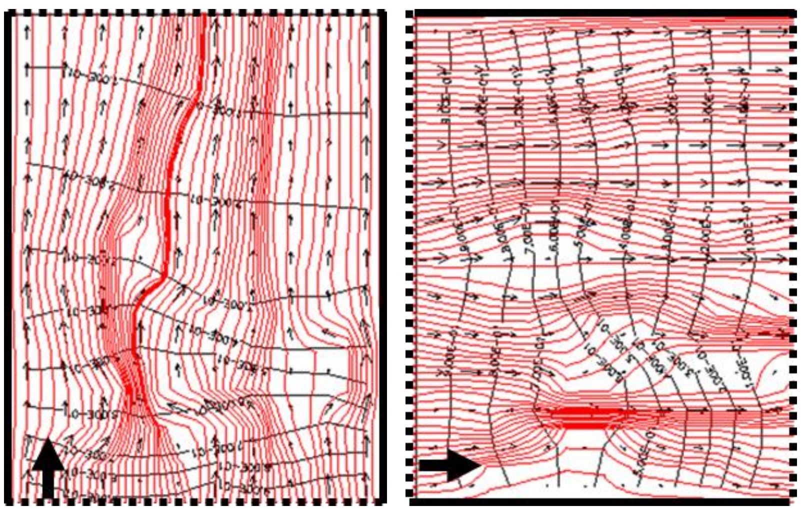

Poederlee Sands

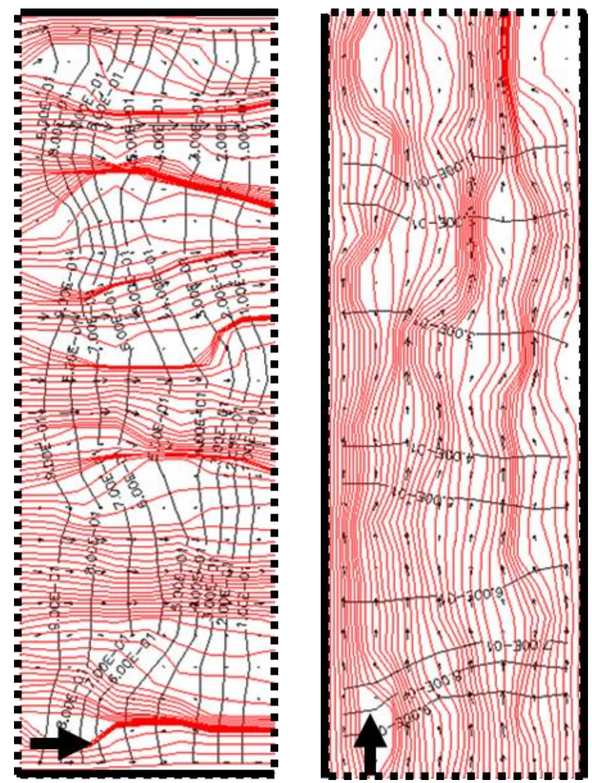

Diest Clayey Sands

Numerical upscaling

ID	Sediment	Permeameter setup		
		$\log_{10}(K_{xx})$	$\log_{10}(K_{zz})$	VANI
c	Ice wedge & cryoturbation structures	-4.15	-5.57	26.42
d	Lommel Sands	-4.19	-4.19	1.00
e	Mol Sands	-3.64	-3.60	0.92
f	Top Poederlee Formation	-3.88	-5.31	26.71
g	Bottom Poederlee Formation 1	-4.80	-6.23	26.86
h	Bottom Poederlee Formation 2	-3.84	-4.02	1.51
j	Kasterlee Sands	-3.86	-3.85	0.98
k	Kasterlee Clay	-4.13	-5.71	38.31
l	Clayey top Diest Formation	-3.56	-3.88	2.08
m	Diest Sands	-4.06	-4.14	1.21
n	Bolderberg Sands 1	-3.81	-3.84	1.07
o	Bolderberg Sands 2	-3.86	-3.88	1.05

Contents

Conclusions

- A handheld air permeameter is an efficient tool to characterise hydraulic conductivity
- It offers access to spatial variability on scales that are not feasible by classical core-based techniques
- Validation shows that the K_s estimates are within one order of magnitude from the laboratory analyses results
- Complex stratigraphical settings can be effectively characterised if outcrops of the different components are available

Acknowledgements

- The authors thank Katrijn Vandersteen and Koen Vos for their assistance during the field work.
- Sibelco and Terca Nova are acknowledged for the permission to access their quarries. Via Kempen is acknowledged for the permission to access the Kempense Noord-Zuidverbinding road construction yard.

Centimeter-scale secondary information on hydraulic conductivity using a hand-held air permeameter on borehole cores

Rogiers, B.[1,2*], Winters, P.[3], Huysmans, M.[2], Beerten, K.[1], Mallants, D.[3], Gedeon, M.[1], Batelaan, O.[2,4] & Dassargues, A.[2,5]

[1] Institute for Environment, Health and Safety, Belgian Nuclear Research Centre (SCK•CEN), Boeretang 200, BE-2400 Mol, Belgium. // [2] Dept. of Earth and Environmental Sciences, K.U.Leuven, Celestijnenlaan 200e - bus 2410, BE-3001 Heverlee, Belgium. // [3] Groundwater Hydrology Program, CSIRO Land and Water, Waite Road - Gate 4, Glen Osmond SA 5064, Australia. // [4] Dept. of Hydrology and Hydraulic Engineering, Vrije Universiteit Brussel, Pleinlaan 2, BE-1050 Brussels, Belgium. // [5] Hydrogeology and Environmental Geology, Dept. of Architecture, Geology, Environment and Civil Engineering (ArGEnCo) and Aquapole, Université de Liège, B.52/3 Sart-Tilman, BE-4000 Liège, Belgium.

*Corresponding author: brogiers@sckcen.be

Introduction

- Saturated hydraulic conductivity (K_s)
  - Is one of the most important parameters
  - determining groundwater flow and contaminant transport
  - in both unsaturated and saturated porous media
- Small-scale variability of K_s is key to obtain effective transport parameters and to explain K_s measurements or inverse estimates at the larger scale
- ~350 m of borehole core is available at Mol/Dessel, Belgium (Fig. 1; Beerten et al. 2010)
  - sediments of Miocene to Pleistocene age, marine to continental origin
  - sand to clayey sand with distinct clay lenses, with varying glauconite content
  - 2 samples each 2 meters with K_s from constant head permeameter tests in the lab
  - K_s range of 7 orders of magnitude
- Thin slabs separated from the cores are analysed in this study (Fig. 1)

Figure 1: Core sampling at SCK•CEN: a) schematic of slab removal from main core, b) incision is made in main core to the appropriate depth for slab removal, c) 100 cm³ steel core for hydraulic conductivity determination in the lab, d) steel core inserted in core material, e) vacuum sealing of main core for long-term storage, f) display of core slabs for geological description.

Methods

- Measurements
  - Use of the TinyPerm II hand-held air permeameter device (Fig. 2; New England Research & Vindum Engineering 2011)
  - > 5000 measurements on the dry borehole core slabs at 5 cm resolution, performed within 5 days (Figs. 3 & 6)
  - Equation of Loll et al. (1999) to convert air permeability to a K_s estimate, since perfect agreement between intrinsic permeability estimated from measurement of air and water flow cannot be expected
  - Additional measurements to quantify measurement error and operator influence (Fig. 4)
- Calibration with the lab K_s measurements with a linear mixed-effects model, with random effects for both the stratigraphy and borehole factors (Fig. 5)
- Spatial analysis
  - Variography for the lab measurements and air permeameter estimates after standardisation
  - Fitting an intrinsic model of co-regionalisation (Goovaerts 1997)
  - Interpolation of lab K_s data with air permeameter estimates as secondary variable
  - Leave-two-out cross-validation to quantify the predictive uncertainty on K_s, and the accuracy gain with using the secondary data (samples at a distance of about 10 cm are left out together)

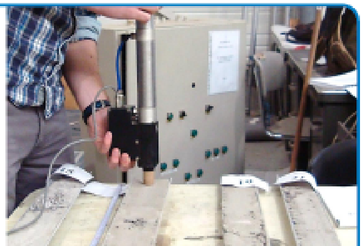

Figure 2: Performing air permeameter measurements on borehole core slabs.

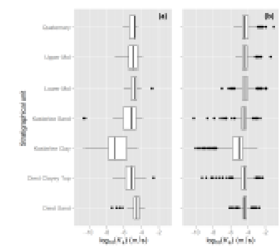

Figure 3: Boxplots of K_s values from a) the lab analysis, and b) the air permeameter K_s estimates (based on Loll et al., 1999), for each of the stratigraphical units. The whiskers extend to the most extreme data point that is no more than 1.5 times the interquartile range from the box.

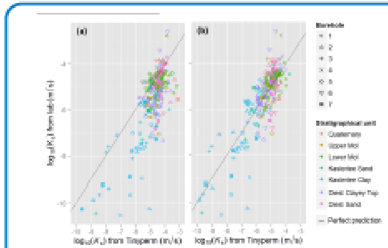

Figure 5: Calibration of the air permeameter K_s estimates (a; using Loll et al., 1999), with laboratory analyses data, by means of a linear mixed effects model with a random effect for each stratigraphical unit and each borehole (b).

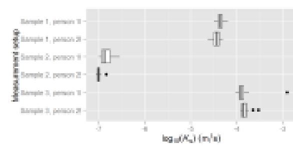

Figure 4: Repeated measurements and operator influence.

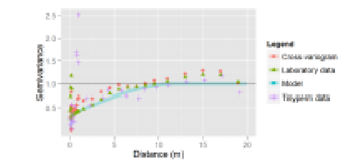

Figure 6: Experimental direct and cross-variograms of the standardised data, and the corresponding intrinsic model of coregionalisation, consisting of a short (0.4 m) and long range (12 m) spherical variogram model.

Results

- The relative differences between the stratigraphical units corresponds to the lab analyses observations (Fig. 3)
- A systematic bias and smaller range of K_s values is predicted using the equation from Loll et al. (1999)
- Measurement error as well as the systematic bias introduced by the operator are small compared to the intrinsic K_s variability (compare Figs. 3 & 4)
- Correlation between lab measurements and air permeability estimates is 0.74 and increases after calibration to 0.84 (see Fig. 5)
- After standardisation of the data, an intrinsic model of coregionalisation was fitted to the experimental variograms with two nested spherical models (Fig. 6). One for the short range (0.4 m) and one for the long range (12 m).
- Predictions are presented on Fig. 7, and show a lot of small-scale heterogeneity, as well as clear zones of lower K_s values. In the zones for which core slabs were missing, important uncertainty remains, as indicated by the larger confidence intervals.
- Cross-validation results (see Fig. 8)
  - Performance kriging: MSE: 1.13; ME: 0.04; R^2: 0.31
  - Performance co-kriging: MSE: 0.79; ME: -0.02; R^2: 0.71
  - Especially the low K_s range predictions are improved

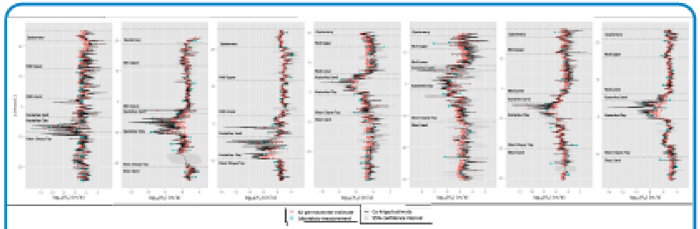

Figure 7: Vertical profiles of K_s values from the lab analyses, the air permeameter K_s estimates after calibration, and the cokriging estimates and 95% confidence interval.

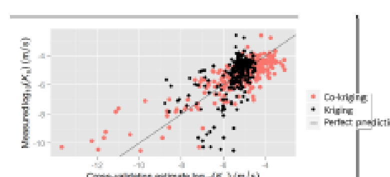

Figure 8: Leave-two-out cross-validation results for both kriging and co-kriging estimation.

Conclusions

- Hand-held air permeameter measurements on undisturbed borehole cores provide a very cost-effective way to obtain high-resolution K_s data
- Even core slabs that have been lying open to air, and have been subject of several investigations during a few years, provide useful information
- Without calibration, reliable relative K_s estimates can be obtained, and equations from literature provide absolute K_s estimates (e.g. Loll et al. 1999)
- Calibration with laboratory measurements improves the accuracy, and is recommended for core slabs of this state

Acknowledgements

The authors are grateful to ONDRAF/NIRAS, the Belgian Agency for Radioactive Waste and Enriched Fissile Materials, for providing the borehole cores and laboratory data. Findings and conclusions in this paper are those of the authors and do not necessarily represent the official position of ONDRAF/NIRAS. Serge Labat and Frans Siegers are acknowledged for their help with handling the borehole cores.

References

Beerten K., Wemaere I., Gedeon M., Labat S., Rogiers B., Mallants D., Salah S. & Leterme B. (2010). Geological, hydrogeological and hydrological data for the Dessel disposal site. Project near surface disposal of category A waste at Dessel – Version 1.- Brussels, Belgium: NIRAS/ONDRAF, 2010.- 273 p.- NIROND–TR 2009–05 E V1.
Goovaerts, P. (1997). Geostatistics for Natural Resources Evaluation (Applied Geostatistics Series) (p. 496). Oxford University Press, USA.
Loll, P., Moldrup, P., Schjønning, P., & Riley, H. (1999). Predicting saturated hydraulic conductivity from air permeability: Application in stochastic water infiltration modeling. Water resources research, 35(8), 2387–2400. American Geophysical Union.
New England Research & Vindum Engineering (2011). TinyPerm II Portable Air Permeameter, User's Manual. Retrieved from http://www.vindum.com/TinyPermManual.pdf on 14-06-2011.

www.sckcen.be
info@sckcen.be
201210_BRogiers

Copyright notice

brogiers@sckcen.be

SCK•CEN
Studiecentrum voor Kernenergie
Centre d'Etude de l'Energie Nucléaire

Stichting van Openbaar Nut
Fondation d'Utilité Publique
Foundation of Public Utility

Registered Office: Avenue Herrmann-Debrouxlaan 40 – BE-1160 BRUSSEL
Operational Office: Boeretang 200 – BE-2400 MOL

Thank you for your attention!
Questions?

References

- Li, L., Zhou, H., & Jaime Gómez-Hernández, J. (2011). A Comparative Study of Three-Dimensional Hydraulic Conductivity Upscaling at the MAcro-Dispersion Experiment (MADE) site, Columbus Air Force Base, Mississippi (USA). Journal of Hydrology, 404(3-4), 278-293. Elsevier B.V. doi:10.1016/j.jhydrol.2011.05.001
- New England Research & Vindum Engineering (2011). TinyPerm II Portable Air Permeameter, User's Manual. Retrieved from http://www.vindum.com/TinyPermManual.pdf on 14-06-2011.
- Zhou, H., Li, L., & Jaime Gómez-Hernández, J. (2010). Three-dimensional hydraulic conductivity upscaling in groundwater modeling☆. Computers & Geosciences, 36(10), 1224-1235.